JACS
JOURNAL OF THE AMERICAN CHEMICAL SOCIETY

Article

pubs.acs.org/JACS

Dissecting Chemical Interactions Governing RNA Polymerase II Transcriptional Fidelity

Matthew W. Kellinger,[†] Sébastien Ulrich,[‡] Jenny Chong,[†] Eric T. Kool,*[,‡] and Dong Wang*[,†]

[†]Skaggs School of Pharmacy and Pharmaceutical Sciences, The University of California, San Diego, La Jolla, California 92093-0625, United States

[‡]Department of Chemistry, Stanford University, Stanford, California 94305-5080, United States

Supporting Information

ABSTRACT: Maintaining high transcriptional fidelity is essential to life. For all eukaryotic organisms, RNA polymerase II (Pol II) is responsible for messenger RNA synthesis from the DNA template. Three key checkpoint steps are important in controlling Pol II transcriptional fidelity: nucleotide selection and incorporation, RNA transcript extension, and proofreading. Some types of DNA damage significantly reduce transcriptional fidelity. However, the chemical interactions governing each individual checkpoint step of Pol II transcriptional fidelity and the molecular basis of how subtle DNA base damage leads to significant losses of transcriptional fidelity are not fully understood. Here we use a series of "hydrogen bond deficient" nucleoside analogues to dissect chemical interactions governing Pol II transcriptional fidelity. We find that whereas hydrogen bonds between a Watson−Crick base pair of template DNA and incoming NTP are critical for efficient incorporation, they are not required for efficient transcript extension from this matched 3′-RNA end. In sharp contrast, the fidelity of extension is strongly dependent on the discrimination of an incorrect pattern of hydrogen bonds. We show that U:T wobble base interactions are critical to prevent extension of this mismatch by Pol II. Additionally, both hydrogen bonding and base stacking play important roles in controlling Pol II proofreading activity. Strong base stacking at the 3′-RNA terminus can compensate for loss of hydrogen bonds. Finally, we show that Pol II can distinguish very subtle size differences in template bases. The current work provides the first systematic evaluation of electrostatic and steric effects in controlling Pol II transcriptional fidelity.

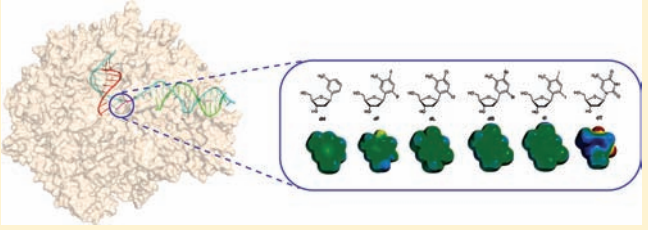

INTRODUCTION

Maintaining a highly faithful readout of genetic information from DNA to RNA during the process of transcription is essential to life. For all eukaryotic organisms, RNA polymerase II (Pol II) is responsible for messenger RNA synthesis from the DNA template. A long-standing question in transcription is how Pol II achieves high transcriptional fidelity, and what chemical interactions play important roles in controlling this fidelity. Mechanistic insights on this subject have been obtained from a combination of structural, genetic, and biochemical studies.[1−18] The high accuracy of Pol II is achieved in three key checkpoint steps: specific nucleotide selection and incorporation, differentiation of RNA transcript extension of a matched over mismatched 3′- RNA terminus, and preferential removal of misincorporated nucleotides from the 3′-RNA end (proofreading).[2,4,6,12,14,15,19−28] In the first step, interaction networks between Pol II residues and the NTP substrate and between template DNA and substrate (including base pairing and base stacking) are all believed to play important roles in substrate selection. Upon binding the correct substrate, the trigger loop of Pol II is switched to a closed active conformation, positioning the incoming NTP and promoting its addition to the RNA 3′ end (Figure 1a). Mutations in the Pol II trigger loop and other active site residues have been shown to diminish transcriptional fidelity greatly.[2,3,11] Second, the differentiation of RNA transcript extension of a matched over mismatched 3′-RNA terminus serves as an additional checkpoint to discriminate nucleotide misincorporation events kinetically. The transcription elongation rate is much slower for a mismatched than a matched 3′-end. This slow extension over the mismatched 3′-end also provides a time window for Pol II proofreading,[14,25−27] which is the third mechanism by which Pol II transcriptional fidelity can be further improved. Misincorporation causes Pol II to move in a "backtracking" mode,[4] in which dinucleotides or short oligomers containing the misincorporated nucleotide are preferentially removed either by Pol II alone (intrinsic cleavage) or by TFIIS-stimulated cleavage of 3′-end RNA residues.[20,29]

In addition, DNA damage to the template adds another important layer of modulation of transcriptional fidelity. In fact, cellular DNA is under continuous attack by both metabolic and environmental agents, resulting in as many as tens of thousands of individual DNA lesions per cell per day.[30] Some types of chemical modifications to nucleotide bases caused by DNA-damaging agents greatly reduce transcriptional fidelity by

Received: March 2, 2012
Published: April 17, 2012

   dx.doi.org/10.1021/ja302077d | J. Am. Chem. Soc. 2012, 134, 8231−8240

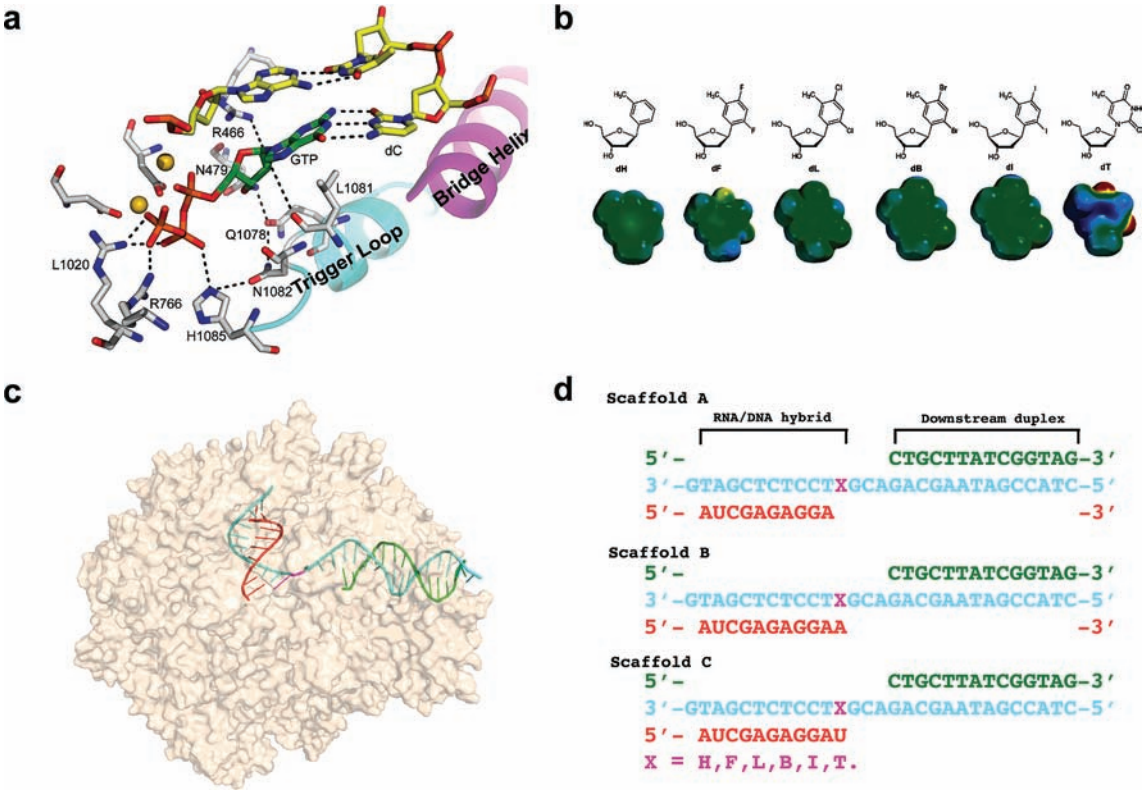

Figure 1. Pol II elongation complexes containing site-specific nonpolar nucleoside analogues. (a) Detailed structure of the active site of the Pol II elongation complex bound with a matched GTP (PDB: 2E2H). The bridge helix and trigger loop are shown in magenta and cyan, respectively. RNA and DNA are shown in yellow and GTP is green. Side chains are shown as sticks. Nitrogen, oxygen, and phosphate atoms are highlighted in blue, red, and orange, respectively. Mg^{2+} ions are shown in gold. (b) The structures of nonpolar nucleoside analogues H, F, L, B, I compared with thymidine (T). (c) Cutaway view of Pol II elongation complex. Pol II is revealed as a tan surface. RNA, template DNA, and non-template DNA are shown in red, cyan, and green, respectively. The nonpolar nucleoside analogue is highlighted in magenta. (d) Scaffold sequences of RNA, template DNA, and nontemplate DNA in this study are depicted in red, cyan, and green, respectively. X refers to H, F, L, B, I, and T.

several orders of magnitude, whereas other modifications/lesions have virtually no effect.[13,31−39] Thus, error-prone transcription bypass of DNA damage, termed transcriptional mutagenesis, may be an important pathway for the generation of mutant proteins and therefore play a role in tumor development.[38]

The molecular basis of how subtle DNA base damage leads to significant losses of transcriptional fidelity, and the chemical interactions governing each individual checkpoint step of Pol II transcriptional fidelity on damaged or undamaged DNA templates, are not fully understood. Here we take a systematic approach to dissect chemical interactions governing Pol II transcriptional fidelity in each checkpoint step. We replace canonical DNA template bases with nonpolar thymine analogues of varied size (Figure 1b).[40,41] These "hydrogen bond deficient" analogues allow us to dissect the roles of electrostatic effects such as hydrogen bonds and of steric effects in controlling Pol II transcriptional fidelity.

RESULTS

For this study we synthesized DNA templates containing five low-polarity thymidine isosteres[40,41] (denoted by H, F, L, B, I) that closely mimic the shape of thymidine but vary by sub-angstrom increments in size (Figure 1b and Supplementary Figures 1−6). As all carbonyl and NH groups are removed, all five analogues are completely deficient in canonical hydrogen bond formation between base pairs.[42] By removing all the strongly polar groups (rather than partial removal), we can examine the effects of sterics in the absence of strong electrostatic effects, and also rule out any possible alternative hydrogen-bonded arrangements such as wobble-type interactions in our analysis. The series is varied in size systematically: the second (F) is nearly identical in size and shape to thymidine, while H is smaller and L, B, and I are increasingly larger. The overall changes in the series are subtle, with only a ∼1.0 Å difference in size across the series. We then assembled active yeast RNA Pol II elongation complexes with template DNA strands containing the site-specific nucleoside analogues (Figure 1c,d). The Pol II elongation complex (scaffold A, Figure 1d) is in the post-translocation state, in which the active site is empty and poised for nucleotide addition.[1,2] The nucleoside analogues were positioned at the +1 site of template DNA, serving as a possible template for a given incoming nucleoside triphosphate. In addition, we also assembled Pol II elongation complexes in scaffolds B and C (Figure 1d) to test RNA transcript extension and TFIIS cleavage. Taken together, this system allowed us to investigate the individual contributions of hydrogen bonds, size, and stacking interactions at every checkpoint step of Pol II transcription fidelity maintenance.

First Checkpoint Step: Nucleotide Selection and Incorporation against Nonpolar Templates. To test whether Pol II can recognize these nonpolar analogues as thymidine during RNA synthesis, we first incubated the Pol II elongation complex (scaffold A) in the presence of 250 μM ATP. Only small amounts of ATP incorporation were observed in the first 5 min for DNA templates containing nucleoside

analogues (H, F, L, B, I), whereas transcripts were already fully extended for DNA template containing thymidine (T) (Figure 2a, 11 nt). With longer incubation (30 min), substantial

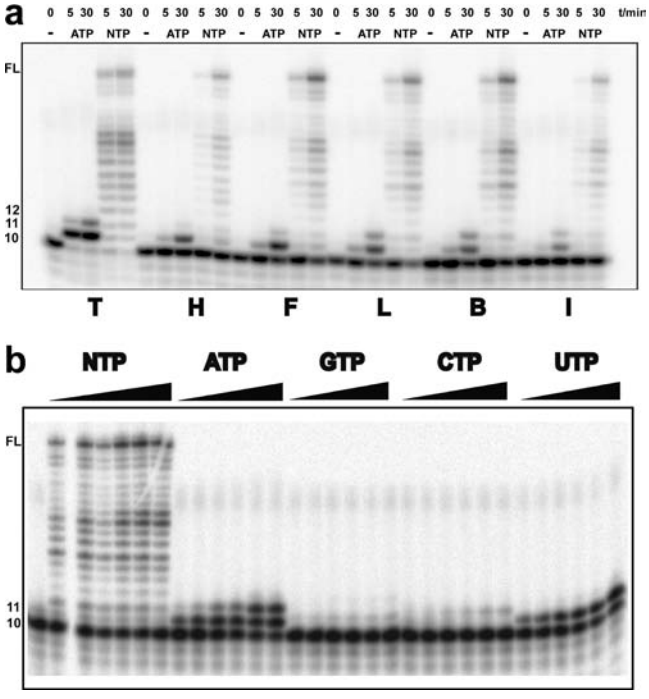

Figure 2. Pol II can use nonpolar nucleoside analogues as DNA templates for nucleotide incorporation and further RNA transcript elongation. (a) The single-base resolution denatured PAGE-urea gel image of RNA transcripts shows nucleotide incorporation and bypass at varied times (0, 5, and 30 min respectively). Aliquots of Pol II elongation complex (40 nM) were mixed with equal volumes of elongation buffer containing 250 μM of NTP mixture or ATP at 22 °C in elongation buffer (20 mM Tris-HCl (pH = 7.5), 40 mM KCl, 5 mM $MgCl_2$). The initial RNA primer (10 nt) was 5′-^{32}P-labeled. The incorporation of ATP or the extension of RNA transcripts with NTP was monitored by the increases in RNA primer length (upper bands). Positions of full-length (FL) RNA transcripts and lengths of short RNA transcripts (products) are shown on the left. (b) Image of representative denaturing PAGE-urea gel of Pol II transcription products using template L in the presence of 25, 50, 100, 200, 500, and 1000 μM of NTP, ATP, GTP, CTP, and UTP, respectively. ATP and UTP are incorporated more efficiently than CTP and GTP.

incorporation was observed with the isostere templates (11 nt). Analogue I (the largest in size) has the lowest incorporation efficiency among the five analogues, whereas F and L, the closest in size to thymidine, exhibit the highest incorporation efficiency. Interestingly, we observed that Pol II can further insert an additional ATP one base downstream to form an A:G mismatched pair when incubated with templates containing L and B, and to a lesser extent F and I, but essentially not with H (Figure 2a,b, 12 nt). A similar mispairing extension also occurs with the natural thymidine template.

To test the substrate selectivity of Pol II with templates containing nucleoside analogues, we incubated Pol II complexes with varied concentrations of ATP, UTP, CTP, and GTP in separate experiments. ATP incorporation efficiency was the highest among the four NTP substrates, whereas almost no detectable CTP was incorporated for all DNA templates (Figure 2b and Supplementary Figure 7). The incorporation efficiencies of UTP and GTP are analogue-specific and quite different from what was seen with the canonical T template. Interestingly, almost no GTP incorporation was observed for H, F, L, B, and I templates, whereas a significant amount of GTP was seen with the natural T template, yielding a wobble pair. On the other hand, substantial amounts of UTP incorporation were observed for F, L, B, I, and natural T templates, but almost no UTP was incorporated with the H template. In summary, for a natural T template, the efficiency of nucleotide incorporation is ATP $\gg$ GTP > UTP $\gg$ CTP, as expected. For the modified templates, the nucleotide incorporation efficiency is ATP $\gg$ UTP > (GTP, CTP) for H template and (ATP, UTP) $\gg$ (GTP, CTP) for the other analogue templates. Overall, these "hydrogen bond deficient" thymidine analogues are processed like thymidine, favoring adenine incorporation, but a lack of canonical hydrogen bonding groups decreases wobble G mispairing and greatly increases U mispairing.

Since ATP and UTP incorporation opposite the nonpolar thymidine analogues is much more efficient than CTP and GTP incorporation, we then measured the specificity constant ($k_{pol}/K_{d,app}$) (second-order rate constant describing the effective rate of substrate binding leading to product turnover) of ATP and UTP incorporation using single-turnover assays. Single-turnover experiments allow direct determination of the principal kinetic parameters k_{pol} (the pseudo-first-order catalytic rate constant) and $K_{d,app}$ (the apparent equilibrium constant for dissociation of nucleotide triphosphate from the Pol II elongation complex) of nucleotide incorporation. The ratio $k_{pol}/K_{d,app}$ is the definition of substrate specificity (it is also termed "catalytic efficiency"). Therefore, the comparison of $k_{pol}/K_{d,app}$ for correct (ATP) and incorrect nucleotide (UTP) incorporations gives a quantitative measurement of the fidelity of Pol II. The nucleotide concentration dependence of product formation data was fit by global simulation analysis to determine maximum rates of nucleotide incorporation (k_{pol}) and apparent dissociation constants ($K_{d,app}$) governing nucleotide binding (Supplementary Figure 8 and Table 1).

Correct nucleotide incorporation on an unmodified T template (ATP:T) yielded the fastest rate of incorporation (k_{pol}) of 750 $\pm$ 210 min^{-1}, and an apparent dissociation constant K_d of 90 $\pm$ 20 μM (Table 1), giving a specificity constant ($k_{pol}/K_{d,app}$) of 8.3 μM^{-1} min^{-1} (Figure 3a). In sharp contrast, analysis of mismatched nucleotide incorporation against the T template (UTP:T) resulted in values of 0.015 $\pm$ 0.003 min^{-1} and 800 $\pm$ 60 μM for k_{pol} and $K_{d,app}$, respectively (Table 1), and a specificity constant of 1.9×10^{-5} μM^{-1} min^{-1} (Figure 3b).

Substituting the thymidine template with its fluorinated isostere (F) altered the kinetics of correct and mismatched NTP incorporation dramatically. The loss of canonical hydrogen bonding leads to a ~5800-fold decrease in k_{pol} (0.13 $\pm$ 0.02 min^{-1}) and a 6-fold decrease in the apparent binding affinity of ATP (540 $\pm$ 30 μM) (Table 1). Therefore, the specificity constant of ATP incorporation for the F template (2.4×10^{-4} μM^{-1} min^{-1}) shows a 3.5×10^4-fold decrease relative to the T template (Figure 3a). On the other hand, mismatch UTP incorporation against the F template resulted in a ~13-fold increase in k_{pol} but no effect on $K_{d,app}$. The specificity constant for UTP:F incorporation is 2.5×10^{-4} μM^{-1} min^{-1}, a value ~13-fold higher than that of UTP:T incorporation. Similar findings were observed for F, B, and L templates and are listed in Table 1. In contrast, the specificities of ATP incorporation for the largest (I) and the smallest (H)

dx.doi.org/10.1021/ja302077d | J. Am. Chem. Soc. 2012, 134, 8231−8240

Table 1. Kinetics of Nucleotide Incorporation Opposite T and Nonpolar Templates

template base	NTP	k_{pol} (min^{-1})	$K_{d,app}$ (μM)	$k_{pol}/K_{d,app}$ (10^{-5} μM^{-1} min^{-1})	discrimination[a]
T	ATP	750 ± 210	90 ± 20	(8.3 ± 3.0) × 10^5	(4.4 ± 1.9) × 10^5
	UTP	0.015 ± 0.003	800 ± 60	1.9 ± 0.4	
H	ATP	0.054 ± 0.006	580 ± 100	9.3 ± 1.9	100 ± 40
	UTP	0.0005 ± 0.0001	560 ± 160	0.09 ± 0.03	
F	ATP	0.13 ± 0.02	540 ± 30	24 ± 4	1.0 ± 0.3
	UTP	0.19 ± 0.04	760 ± 60	25 ± 6	
L	ATP	0.16 ± 0.04	590 ± 60	27 ± 7	1.0 ± 0.4
	UTP	0.18 ± 0.04	660 ± 60	27 ± 7	
B	ATP	0.18 ± 0.06	650 ± 270	28 ± 15	1.2 ± 0.7
	UTP	0.16 ± 0.04	680 ± 100	24 ± 7	
I	ATP	0.08 ± 0.02	730 ± 200	11 ± 4	0.9 ± 0.6
	UTP	0.14 ± 0.06	1100 ± 500	13 ± 8	

[a]Discrimination = $(k_{pol}/K_{d,app})_{ATP}/(k_{pol}/K_{d,app})_{UTP}$.

template bases are similar, and both are ~2 fold lower than that for F template. However, the specificity of UTP incorporation for these two is quite different, being relatively high for I (1.3×10^{-4} μM^{-1} min^{-1}) and very low for H (9×10^{-7} μM^{-1} min^{-1}) (Table 1).

Comparison of specificities for the "matched" nucleotide (ATP) and the mismatched one (UTP) allows a measure of nucleotide selectivity (discrimination). The relative specificities governing ATP versus UTP incorporation against the T template show a 4.4×10^5-fold discrimination (Figure 3c). In sharp contrast, the discrimination of ATP over UTP for F, L, B, I templates is near 1.0, because of the comparable $k_{pol}/K_{d,app}$ for both ATP and UTP, respectively, for these templates (see Table 1). Therefore, there is no nucleotide selectivity between the ATP and UTP for F, L, B, I templates (Figure 3c). Interestingly, the smallest analogue (H) shows moderate discrimination (~100-fold) for ATP over UTP because of the low efficiency of UTP incorporation (Figure 3c), indicating the effect of size of template base on nucleotide selection.

Second Checkpoint Step: Pol II Bypasses beyond the Nucleoside Analogue Site. To test the ability of Pol II to elongate the growing RNA strand beyond nonpolar analogues, we then incubated Pol II complexes with varied concentrations of mixed nucleoside triphosphates. No bands indicative of significant pausing after the +1 position were observed for any of the analogues, and full-length RNAs were seen with slight banding patterns similar to that with the natural thymidine template. Substantial amounts of bypassed full-length RNA transcripts were obtained for the analogue templates in prolonged incubation (Figure 2 and Supplementary Figure 7a), indicating that the efficiency of continued extension is much higher than the first nucleotide incorporation, as described above. Templates H and I (the smallest and largest analogues, respectively) show the lowest bypass efficiency, and intermediate-sized L has the highest efficiency among the five analogues.

To further investigate the extension kinetics beyond nonpolar template bases, we then measured the specificities of subsequent nucleotide incorporation beyond the nonpolar thymidine analogue site with Pol II elongation complexes in scaffolds B or C, respectively. The goal was to evaluate the contributions of hydrogen bonding and base stacking at the 3′ terminus of the primer to the next nucleotide incorporation. We found that CTP incorporation following the correct A:T base pair yields a k_{pol} value of 450 ± 20 min^{-1} and an apparent dissociation constant ($K_{d,app}$) of 52 ± 5 μM, resulting in a specificity constant of 8.7 μM^{-1} min^{-1} (Table 2). In sharp contrast, replacing the 3′ RNA terminus with a U:T mismatch results in significantly slower CTP incorporation kinetics with a ~1700-fold decrease in k_{pol} (0.26 ± 0.05 min^{-1}), ~58-fold decrease in $K_{d,app}$ (3000 ± 700 μM), and ~10^5-fold decrease in $k_{pol}/K_{d,app}$ (8.7×10^{-5} μM^{-1} min^{-1}) (Table 2).

Intriguingly, replacement of the correct A:T base pair with the nonpolar analogue pairs of A:F and A:I at the 3′-RNA terminus does not result in a significant change in specificity constant for CTP incorporation (Figure 4a). The A:F and A:I scaffolds produce CTP specificity constants of 5.0 and 9.5 μM^{-1} min^{-1}, respectively (Table 2). Even more surprisingly, CTP incorporation on the U:F or U:I template results in a 250- and 1030-fold increased specificity constant compared with U:T, respectively (Figure 4b). Consequently, the discrimination of a matched over a mismatched 3′-RNA terminus decreases significantly as a result of halogen analogue substitution. Incorporation of CTP on the A:T template is favored 10^5-fold over the U:T mismatch (Figure 4c). This value decreases with substitution of the fluorine analogue so that CTP incorporation on the A:F scaffold is only favored ~2×10^2-fold compared with the U:F scaffold (Figure 4c). Larger iodine substitution further decreases the efficiency difference to only ~10^2-fold for A:I compared with U:I. Notably, these decreases in extension discrimination are mainly caused by an increase in extension efficiency from a mismatched 3′-end (U:X, X = T, F, or I), instead of a decrease in extension efficiency from a matched 3′-end (A:X). Taken together, these findings suggest that hydrogen bonding ability is not required for efficient transcript extension from a matched 3′-RNA end. In sharp contrast, however, the ability to form strong hydrogen bonds is critical for discrimination against mismatched pairs (in this case a U-T wobble pair).

Third Checkpoint Step: Pol II Proofreading of RNA Transcripts Opposite Nonpolar Analogues. Finally, we investigated the role of hydrogen bonds and base pair sterics in

dx.doi.org/10.1021/ja302077d | J. Am. Chem. Soc. 2012, 134, 8231−8240

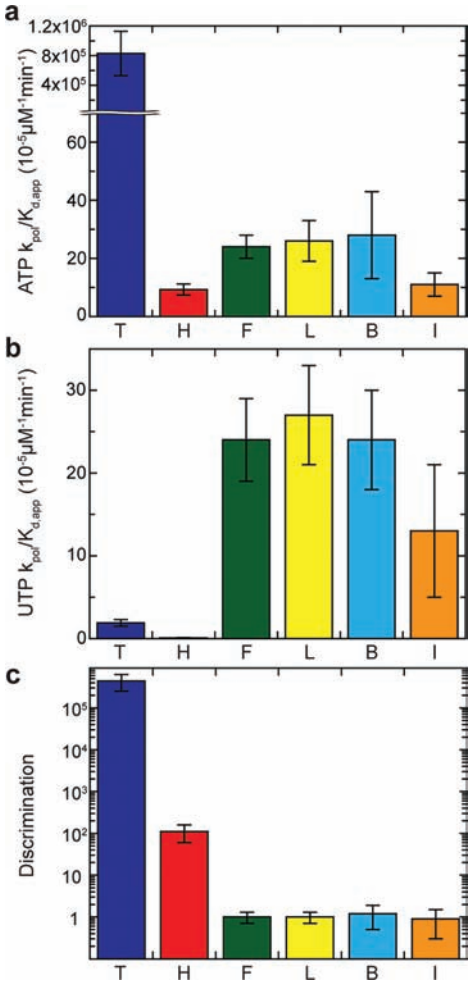

Figure 3. Nonpolar template substitutions alter nucleotide incorporation specificity and discrimination. Specificity constants governing nucleotide incorporation for the correct nucleotide, ATP (a), and a mismatched nucleotide, UTP (b), for each of the nonpolar template analogues. (c) Nucleotide discrimination for ATP over UTP incorporation. Data for T, H, F, B, L, and I are shown in blue, red, green, yellow, cyan, and orange, respectively. All error bars (standard deviation) are derived from three experiments.

controlling backtracking and Pol II proofreading activity. We performed intrinsic cleavage (by Pol II alone) and TFIIS-stimulated cleavage assays using scaffold B and C in the absence of NTP. Experiments showed that the intrinsic cleavage is too slow to be measured accurately even in the presence of 50 mM $MgCl_2$. We therefore focused on TFIIS-stimulated cleavage, which is much faster. As expected, the scaffold B containing a matched 3′-RNA end (A:T) results in the slowest cleavage rate of 0.6 ± 0.1 min^{-1} (Figure 5a). Intriguingly, template substitutions of the smallest nonpolar analogues A:H and A:F produce faster cleavage rates of 6.4 ± 0.7 and 4.4 ± 0.6 min^{-1}, respectively (Figure 5a). In contrast, increasingly larger substitutions of A:L, A:B, and A:I result in cleavage rates similar to the natural A:T template (1.2 ± 0.2, 0.6 ± 0.1, and 1.0 ± 0.2 min^{-1}, respectively) (Figure 5a).

As expected, the scaffold C containing a 3′-RNA U:T mismatch results in a much higher cleavage rate of 7.3 ± 1.6 min^{-1} (Figure 5b). Interestingly, U:H and U:F scaffolds produce similar fast cleavage rates of 8.2 ± 1.3 and 7.8 ± 1.5 min^{-1}, respectively, whereas scaffolds containing U:L, U:B, and U:I each result in slower cleavage rates of 2.6 ± 0.8, 2.3 ± 0.4, and 2.4 ± 0.6 min^{-1}, respectively (Figure 5b).

The templates are thus divided into three groups based on their pattern of cleavage rate: (1) T template; (2) H and F templates; and (3) L, B, and I templates. For T template, the preferential high cleavage rate of U:T mismatched 3′-end over A:T matched 3′-end contributes to an 12-fold increase in Pol II transcriptional fidelity (Table 3). For H and F templates, the cleavage rates for matched and mismatched scaffolds are both high, abolishing the preferential cleavage pattern observed in the natural hydrogen bonded template (Table 3). For L, B, and I templates, the cleavage rates for both matched and mismatched terminal pairs are low and also lead to a loss of preferential proofreading (Table 3).

DISCUSSION

The current experiments provide the first systematic evaluation of electrostatic and steric effects in controlling Pol II transcriptional fidelity in each checkpoint step of transcription. We employed a series of five nonpolar thymidine analogues of varied size to evaluate both the effects of electrostatics (in the form of Watson−Crick hydrogen bonds) and sterics in each of these steps. Overall, the results show that the checkpoints vary greatly in their dependence on these factors, with some steps highly dependent on a strong and correct pattern of hydrogen bonds, and others showing very little dependence on these interactions but reflecting a strong influence of steric and stacking effects instead.

In the first checkpoint of Pol II transcriptional fidelity (nucleotide selection), hydrogen bonding and base stacking between the template base and incoming NTP are proposed to provide an initial selection mechanism that induces a conversion of the Pol II trigger loop to a closed conformation, further aligning catalytic residues for correct nucleotide incorporation.[2,43] Conversely, mismatched nucleotides entering the active site do not form correct Watson−Crick hydrogen

Table 2. Kinetics of Subsequent Nucleotide Extension of a Matched or Mismatched 3′-Terminus

				relative extension efficiency	
3′-terminal base pair	k_{pol} (min^{-1})	$K_{d,app}$ (μM)	$k_{pol}/K_{d,app}$ [a] (μM^{-1} min^{-1})	template modification[b]	3′-RNA mismatch[c]
A:T	450 ± 20	52 ± 5	8.7 ± 0.9	1 ± 0.1	(1.0 ± 0.3) × 10^5
A:F	29 ± 3	5.8 ± 0.7	5.0 ± 0.8	0.6 ± 0.1	230 ± 50
A:I	39 ± 4	4.1 ± 0.6	9.5 ± 1.7	1.1 ± 0.2	110 ± 40
U:T	0.26 ± 0.05	3000 ± 700	(8.7 ± 2.6) × 10^{-5}	1 ± 0.3	–
U:F	10.4 ± 0.7	470 ± 70	(2.2 ± 0.4) × 10^{-2}	250 ± 90	–
U:I	10 ± 2	110 ± 30	0.09 ± 0.03	1030 ± 460	–

[a]Specificity constant = $k_{pol}/K_{d,app}$. [b]Template modification relative extension efficiency = $(k_{pol}/K_{d,app})_{modified\ template}/(k_{pol}/K_{d,app})_{T\ template}$. [c]3′-RNA mismatch relative extension efficiency = $(k_{pol}/K_{d,app})_{A:X}/(k_{pol}/K_{d,app})_{U:X}$.

dx.doi.org/10.1021/ja302077d | J. Am. Chem. Soc. 2012, 134, 8231−8240

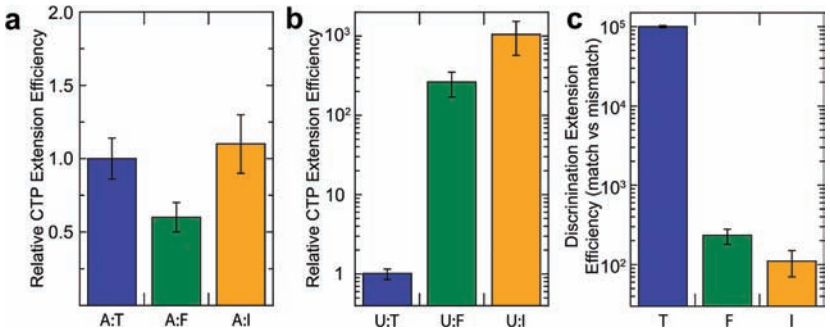

Figure 4. Subsequent nucleotide incorporation beyond matched and mismatched 3′-RNA terminus. Specificity constants for subsequent nucleotide incorporation following either a matched (a) or mismatched (b) 3′-RNA terminus. (c) Nonpolar substitutions decrease the relative discrimination for nucleotide extension. Data for T, F, and I are shown in blue, green, and orange, respectively. All error bars (standard deviation) are derived from three experiments.

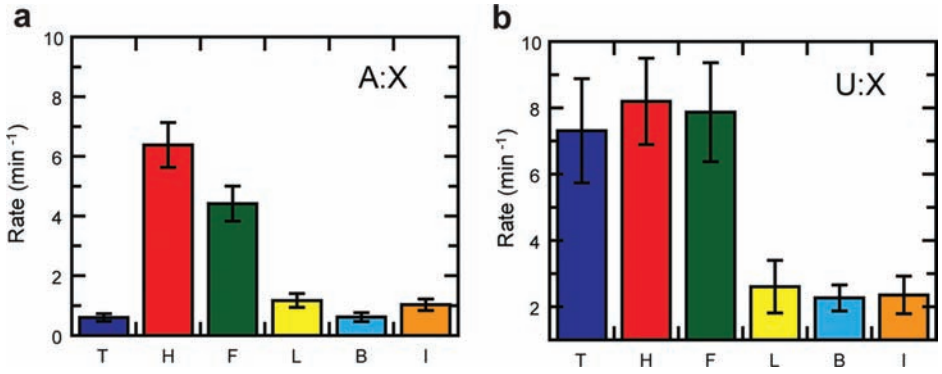

Figure 5. Nonpolar template substitutions alter TFIIS-mediated cleavage kinetics. TFIIS cleavage scaffolds containing adenosine (a) or uracil (b) at the 3′-RNA terminus paired with various nonpolar analogues. Data for T, H, F, B, L, and I are shown in blue, red, green, yellow, cyan, and orange, respectively. All error bars (standard deviation) are derived from three experiments.

Table 3. Nonpolar Template Substitution Effects on TFIIS-Mediated Cleavage

template	3′-RNA nucleotide	cleavage rate (min^{-1})	fidelity contribution[a]
T	A	0.6 ± 0.1	
	U	7.3 ± 1.6	12 ± 3
H	A	6.4 ± 0.7	
	U	8.2 ± 1.3	1.3 ± 0.2
F	A	4.4 ± 0.6	
	U	7.8 ± 1.5	1.8 ± 0.4
L	A	1.2 ± 0.2	
	U	2.6 ± 0.8	2.2 ± 0.8
B	A	0.6 ± 0.1	
	U	2.3 ± 0.4	3.8 ± 0.9
I	A	1.0 ± 0.2	
	U	2.4 ± 0.6	2.4 ± 0.8

[a]Fidelity Contribution = $(k_{TFIIS})_{U:X}/(k_{TFIIS})_{A:X}$.

bonds and are therefore discriminated against. Indeed, we find that correct ATP incorporation against the natural T template is much more efficient than that for F template (~3.5×10^4-fold, Table 1). This finding confirms that for Pol II, hydrogen bonds between a Watson–Crick base pair play an important role in ensuring efficient incorporation of the correct NTP. Notably, the fact that Pol II is able to utilize these hydrogen bond deficient analogues as active templates for preferential ATP incorporation over CTP and GTP misincorporation also suggests basal contributions of template size, shape, and base stacking in nucleotide selection. Interestingly, analogue substitution of the template base has a drastic effect on correct nucleotide k_{pol} values (4.2×10^3- to 1.4×10^4-fold) (Table 1), whereas it only results in a 6- to 8-fold reduction in apparent binding affinity. Thus, the reduction in $k_{pol}/K_{d,app}$ is more attributable to decreased incorporation rates rather than weakened substrate binding. This suggests that hydrogen bonds may play a greater role in correct positioning of the incoming NTP for chemical reaction than in the binding of the incoming nucleotide.

The lack of canonical hydrogen bonding groups yields striking differences in nucleotide selectivity for the thymidine analogues. The natural T template directs small but substantial amounts of G or U misincorporation, presumably forming G:T or U:T wobble base pairs. In sharp contrast, essentially no G incorporation was observed for all five nonpolar analogue templates. As G is the most strongly solvated base (see ref 44 and references cited therein), we hypothesize that G is excluded at least in part by the high cost of desolvation when paired against a nonpolar base. A similar effect has been observed in DNA polymerases,[44−46] where G is also the least efficient pairing partner for the analogues. Steric reasoning also argues against G incorporation: while the analogues resemble 5-methylcytosine to some degree by virtue of a single ring and presence of the 5-methyl group, these compounds possess a C-3 proton that is absent in cytosine. This proton (which is

dx.doi.org/10.1021/ja302077d | J. Am. Chem. Soc. 2012, 134, 8231−8240

directly analogous to the N-3 proton of thymidine) is expected to block pairing with G by presenting extra steric bulk in the center of the base pair.

Interestingly, our data show that Pol II can incorporate UTP opposite the nonpolar analogues with efficiency 10-fold higher than that for the T template. This clearly shows that Pol II requires the hydrogen bonding groups of thymidine to discriminate against U misincorporation. A possible explanation is that the wobble geometry enforced by the hydrogen bonding constraints of a U:T pair is highly disfavored for nucleotide addition by this enzyme, whereas the U-F pair may not be constrained to adopt this geometry. This is a remarkable difference from DNA polymerases. For example, DNA polymerase I shows relatively high discrimination against the analogous dTTP misincorporation opposite the nonpolar thymidine analogues.[40]

Nonpolar analogue substitutions of the template base lead to a significant loss of Pol II nucleotide discrimination of ATP over UTP by ~10^5-fold. The absence of mismatch discrimination for the F, L, B, and I analogues is the result of a large reduction in Pol II specificity for correct ATP (~10^4- to 10^5-fold) contrasted with the small increase in specificity for mismatched UTP specificity (~10-fold) for these analogues. These results suggest that hydrogen bonding is more critical for correct nucleotide selection than mismatch rejection. Structurally, proper hydrogen bonding between the incoming NTP and template may affect the Pol II conformational change or the final position of active site residues to aid in catalysis. Studies to investigate the structural basis of how incoming ATP and UTP are accommodated with nonpolar template bases in the Pol II active site are planned for the future.

In our comparison of ATP incorporation against all five analogues, we further show that the Pol II active site can distinguish sub-angstrom size differences in the template DNA base. ATP incorporation opposite the mid-sized analogue templates (F, L, and B) by Pol II is more efficient than that for slightly smaller (H) and larger template (I) bases. However, the magnitude of this selectivity is much smaller than that for most DNA polymerases, which have shown as much as 2−3 orders of magnitude difference in efficiency across the size series.[45,47−52] This suggests that Pol II has a smaller reliance on steric gating and a larger reliance on hydrogen bonding than A-family DNA polymerases. Interestingly, a similar effect has been noted with Y-family DNA polymerases,[50−52] which also appear to be strongly dependent on strong Watson−Crick hydrogen bonds for nucleotide incorporation. For example, Dpo4 polymerase has a specificity constant for dATP insertion opposite F that is >5000-fold lower than opposite T,[53] and studies with variably sized template bases showed only a relatively small difference in efficiency with changes in template base size.[52] In general, an inverse correlation between the rigidity of DNA polymerase active sites and the reliance on Watson−Crick hydrogen bonds in initial nucleotide selection has been observed.[45,47,52−55] It remains to be seen how different RNA polymerases may vary, but the current results suggest that RNA Pol II has an active site that is considerably less rigid than high-fidelity replicative DNA polymerases. The structure of RNA Pol II (2E2H) reveals an active site that is sterically more open than high-fidelity T7 DNA polymerase (1T7P), and lacks a steric gate for ribose discrimination.[2,54]

The finding that analogue substitutions at the template base abolish mismatch discrimination opposite UTP raises an interesting question of how misincorporated UTP affects subsequent nucleotide incorporation and extension. It has been well documented that the extension of the RNA transcript from a correctly matched 3′-end is much more efficient than mismatched 3′-end by Pol II. However, it was unclear whether this correct matching was defined in the functional sense as a canonically hydrogen-bonded pair, or simply the size and shape of a Watson−Crick pair. Intriguingly, our finding with F and I analogues shows similar specificity constants for next nucleotide insertion regardless of nonpolar analogue substitution at the template −1 position (the position that is 1 bp upstream of the template base at active site). This finding suggests that the hydrogen bonding between a Watson−Crick base pair at the −1 position is dispensable for subsequent nucleotide extension. Instead, shape and base stacking play a dominant role in ensuring efficient extension from A:X pairs (X = T, F, or I).

On the other hand, we find that extension from a mismatched 3′-RNA terminus is very sensitive to nonpolar analogue substitution at the template −1 position. Intriguingly, the $k_{pol}/K_{d,app}$ for the next nucleotide extension from a U:T pair is 250-fold lower than that from a U:F pair. This suggests that hydrogen bonding may play an important role in recognition of a wobble U:T mismatch and constrains the incoming UTP in a conformation that is poorly poised for subsequent nucleotide addition. The hydrogen bond-deficient F analogue may lack the strong structural constraint of wobble geometry and therefore shows a significant increase of $k_{pol}/K_{d,app}$. Substitution with the large I analogue further increases the efficiency by 4-fold, which may be due to the fact that the U:I pair likely approaches the size of a natural pyrimidine-purine pair.

As a result of these combined effects, the absence of hydrogen bonding at the 3′-RNA terminus with analogue substitution decreased mismatch recognition. These results suggest that hydrogen bonding is not needed for efficient extension from a Watson−Crick pair at 3′-RNA terminus, but is critical for disallowing the extension from a mismatched terminus. We find that the absence of hydrogen bonding increases the probability of continued polymerization over a mismatched base pair. In general, the lack of apparent pausing beyond a nonpolar template base also suggests that Pol II has no strong minor groove interactions with the DNA template strand beyond the +1 site, which might normally interact with hydrogen bond acceptors at position 2 of pyrimidines. This is different from some DNA polymerases, which show pausing beyond the incipient base pair as a result of multiple minor groove hydrogen bonds between the enzyme and both DNA strands.[54−61]

Finally, we investigated the last checkpoint step of Pol II transcriptional fidelity: Pol II proofreading through preferential backtracking and cleavage of mismatches at the RNA 3′ end. Our results show that both hydrogen bonding and possibly base stacking interactions contribute to Pol II capability for proofreading misincorporation. As we have shown, correct hydrogen bonding (A:T) at the 3′-end prevents backtracking and TFIIS-mediated cleavage, whereas mismatched (U:T) at the 3′-end favors backtracking and leads to a faster cleavage rate. Substitution with hydrogen bond-deficient analogues H and F resulted in a faster cleavage even in matched base pairs with A (Figure 5a). This establishes that hydrogen bonds play an important role in governing proofreading, possibly by slowing the fraying of the terminus and preventing RNA backtracking. A similar effect was seen previously for 3′ end proofreading by the Klenow fragment of DNA Pol I.[62] Interestingly, substitution with the larger analogues (L, B, I)

dx.doi.org/10.1021/ja302077d | J. Am. Chem. Soc. 2012, 134, 8231−8240

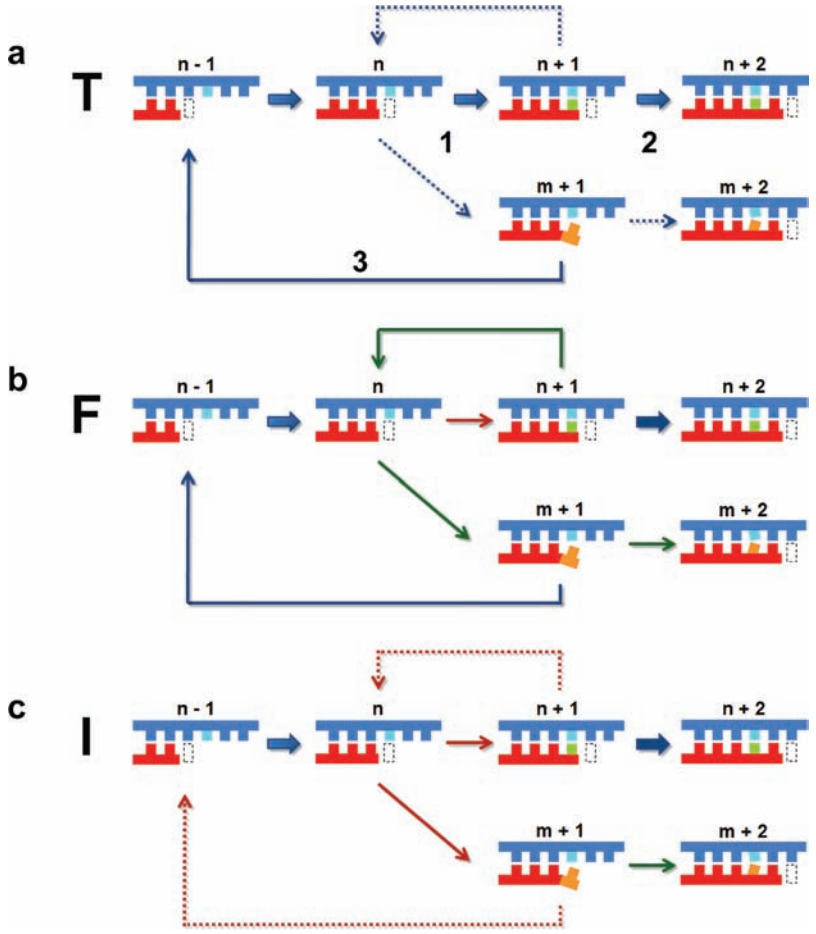

Figure 6. Nonpolar analogues affect the three key checkpoint steps of Pol II transcription fidelity. Scheme of different states of RNA/DNA hybrid within the Pol II active site during the transcription elongation along T template (a), F template (b), and I template (c). Three key checkpoint steps for Pol II transcription fidelity are depicted: (1) nucleotide selection and incorporation, (2) RNA transcript extension, and (3) proofreading. DNA and RNA strands in Pol II transcribing complex are shown in blue and red. The matched and mismatched nucleotides, and their template base are shown in green, orange, and cyan, respectively. Correct incorporation and misincorporation are depicted with n and m, respectively. The positions of 3′-end of matched (n) or mismatched (m) RNA are depicted as registers of $n-1$, n, $n+1$, $n+2$, $m+1$, and $m+2$, respectively. The position of next nucleotide addition is shown in a dotted box. The width of the solid lines corresponds to the rates. The dotted line indicates a very slow reaction. Increase and decrease of rates are shown in green and red, respectively.

resulted in retarded proofreading, giving rates as slow as that for the complex with a matched A:T 3′-end. It is known that these analogues have base stacking ability considerably greater than all natural DNA bases;[63,64] thus, the increased base stacking interactions may compensate for loss of hydrogen bonds at the terminus, slowing fraying and shifting the equilibrium in favor of continued polymerization. Overall, the absence of hydrogen bonding and/or weak base stacking both appear to promote RNA backtracking.

Taken together, the comparison between the results obtained from the naturally substituted T template and nonpolar F template allows us to evaluate the role of hydrogen bonds in each step of transcriptional fidelity (Figure 6). Loss of hydrogen bonding with the template base leads to a significant decrease in correct NTP incorporation, an increase of NTP misincorporation and extension from a mismatched 3′-end, and an increase of cleavage rate from a matched 3′-end, respectively. Similarly, the comparison between variably sized analogues is also instructive: for example, the different results obtained with the F and I templates allows us to assess the role of increased size and base stacking in each step of transcriptional fidelity (Figure 6). Increased size and base stacking at DNA template leads to a universal decrease in NTP incorporation and cleavage, and an increase in extension from a mismatched 3′-end, respectively.

These results provide a framework for understanding the chemical interactions governing Pol II transcriptional fidelity and how DNA damage alters such interactions, resulting in a change of transcriptional fidelity. It would be interesting in the future to expand our research to other structurally related multi-subunit RNA polymerases such as prokaryotic bacterial RNA polymerase and eukaryotic RNA polymerases I and III. Since the nonpolar analogues can be incorporated into biologically active DNAs,[40,65] they may be useful in the future as tools for studying transcription dynamics and fidelity in the cellular context as well.

EXPERIMENTAL SECTION

Preparation of DNA Template Containing Nonpolar Nucleosides Isosteres. The DNA template used in transcription is shown as follows:

5′-CT ACC GAT AAG CAG ACG XTC CTC TCG ATG-3′

dx.doi.org/10.1021/ja302077d | J. Am. Chem. Soc. 2012, 134, 8231−8240

where X refers to nonpolar nucleoside analogues H, F, L, B, I (Figure 1). Detailed procedures for preparation and characterization are given in the Supporting Information.

Pol II Purification and Pol II Elongation Complex Formation. *Saccharomyces cerevisiae* Yeast Pol II enzymes were purified as described.[2] Pol II elongation complexes containing the desired template DNA was prepared essentially as described.[2,4] Briefly, an aliquot of 5′-^{32}P-labeled RNA was annealed with a 2-fold amount of template DNA and non-template DNA to form RNA/DNA scaffold in elongation buffer (20 mM Tris-HCl, pH 7.5, 40 mM KCl, 5 mM $MgCl_2$). An aliquot of annealed scaffold of RNA/DNA was then incubated with a 4-fold excess amount of Pol II at room temperature for 20 min to ensure the formation of a Pol II elongation complex. The Pol II elongation complex is ready for *in vitro* transcription upon addition of equal volume of NTP solution. Scaffolds for the transcription assay are as follow:

RNA/Template DNA/Non-Template DNA:

```
5′- AUCGAGAGGA -3′
3′-GTAGCTCTCCTXGCAGACGAATAGCCATC -5′
5′-                CTGCTTATCGGTAG -3′
```

***In Vitro* Pol II Transcription Elongation Assay.** The assay was carried out as described previously.[10,34,66] Briefly, aliquots of preformed Pol II elongation complex (40 nM) were mixed with equal volumes of elongation buffer containing varied concentrations of NTP mixture (50 μM, 100 μM, 200 μM, 400 μM, and 1 mM, respectively). The reactions were incubated for 5, 30, and 45 min at 22 °C before quenching with stop solution (final concentrations 5 M urea, 44.5 mM Tris-HCl, 44.5 mM boric acid, 26 mM EDTA, pH 8.0, 0.01% Xylene Cyanol and Bromophenol Blue dyes). The transcription products were analyzed by PAGE (15% acrylamide (19:1 bis-acrylamide), 8 M urea, 1x TBE) and quantitated with a Molecular Imager PharosFX Plus system (Bio-Rad) or Typhoon FLA 9000 phosphorimager (GE). All product bands (including the +1 band and longer products) were quantitated for elongation analysis.

Single-Turnover Nucleotide Incorporation Assays. The assay was carried out as described previously.[10,34,66] Briefly, nucleotide incorporation assays were conducted by pre-incubating 100 nM scaffold with 400 nM Pol II for 20 min in elongation buffer at 22 °C. The pre-incubated enzyme:scaffold complex was then mixed with an equal volume of solution containing 40 mM KCl, Tris (pH = 7.5), 10 mM DTT, 10 mM $MgCl_2$, and various 2-fold concentrations of NTP. Final reaction concentrations after mixing were 50 nM scaffold, 200 nM Pol II, 5 mM $MgCl_2$, and various NTP concentrations in elongation buffer. Reactions were quenched at various times by addition of one volume of 0.5 M EDTA (pH = 8.0). Reactions requiring time points shorter than 5 s were quenched using a RQF-3 Rapid Quench Flow (KinTek Corp). Products were separated by denaturing PAGE as previously described.

Single-Turnover TFIIS-Mediated Cleavage Assays. Recombinant transcription factor IIS (TFIIS) was purified as described.[4] Cleavage reactions were performed by pre-incubating Pol II with various scaffolds as previously described. The solution was then mixed with an equal volume on solution containing TFIIS and $MgCl_2$ in elongation. Final reaction conditions were 200 nM Pol II, 50 nM scaffold, 1.5 μM TFIIS, and 5 mM $MgCl_2$. Reactions were quenched at various time by addition of one volume of 0.5 M EDTA (pH = 8.0). Products were separated by denaturing PAGE as previously described.

Data Analysis of Nucleotide Incorporation Kinetics. Data analysis was performed using Global Kinetic Explorer software (KinTek). Alternatively, the time dependence of product formation at a single concentration of NTP was fit by traditional nonlinear regression analysis to an exponential equation using GraFit 5. The NTP concentration dependence of the observed fast rate was then fit to a hyperbolic equation to obtain values for the maximum rate of NTP incorporation (k_{pol}), and an apparent K_d ($K_{d,app}$) governing NTP binding. The specificity constant (k_{cat}/K_m) was then obtained from $k_{pol}/K_{d,app}$. Discrimination was calculated as the ratio of specificity constants governing two different nucleotide incorporation events.

■ ASSOCIATED CONTENT

Ⓢ Supporting Information

Details of analogue and modified DNA template synthesis; MALDI-TOF mass spectrometric data for characterization of DNAs. This material is available free of charge via the Internet at http://pubs.acs.org.

■ AUTHOR INFORMATION

Corresponding Author

dongwang@ucsd.edu; kool@stanford.edu

Notes

The authors declare no competing financial interest.

■ ACKNOWLEDGMENTS

D.W. acknowledges the NIH (GM085136) and start-up funds from Skaggs School of Pharmacy and Pharmaceutical Sciences, UCSD, and Academic Senate Research Award from UCSD. E.T.K. acknowledges the NIH (GM072705) for support. S.U. thanks the French-American Fulbright commission and the Region Alsace for financial support. We thank Drs. E. Peter Geiduschek and James Halpert for their insightful comments and critical reading of the manuscript.

■ REFERENCES

(1) Westover, K. D.; Bushnell, D. A.; Kornberg, R. D. *Cell* **2004**, *119*, 481.

(2) Wang, D.; Bushnell, D. A.; Westover, K. D.; Kaplan, C. D.; Kornberg, R. D. *Cell* **2006**, *127*, 941.

(3) Kaplan, C. D.; Larsson, K.-M.; Kornberg, R. D. *Mol. Cell* **2008**, *30*, 547.

(4) Wang, D.; Bushnell, D. A.; Huang, X.; Westover, K. D.; Levitt, M.; Kornberg, R. D. *Science* **2009**, *324*, 1203.

(5) Kettenberger, H.; Armache, K.-J.; Cramer, P. *Cell* **2003**, *114*, 347.

(6) Kettenberger, H.; Armache, K.-J.; Cramer, P. *Mol. Cell* **2004**, *16*, 955.

(7) Kashkina, E.; Anikin, M.; Brueckner, F.; Pomerantz, R. T.; McAllister, W. T.; Cramer, P.; Temiakov, D. *Mol. Cell* **2006**, *24*, 257.

(8) Zenkin, N.; Yuzenkova, Y.; Severinov, K. *Science* **2006**, *313*, 518.

(9) Koyama, H.; Ueda, T.; Ito, T.; Sekimizu, K. *Genes Cells* **2010**, *15*, 151.

(10) Walmacq, C.; Kireeva, M. L.; Irvin, J.; Nedialkov, Y.; Lubkowska, L.; Malagon, F.; Strathern, J. N.; Kashlev, M. *J. Biol. Chem.* **2009**, *284*, 19601.

(11) Kireeva, M. L.; Nedialkov, Y. A.; Cremona, G. H.; Purtov, Y. A.; Lubkowska, L.; Malagon, F.; Burton, Z. F.; Strathern, J. N.; Kashlev, M. *Mol. Cell* **2008**, *30*, 557.

(12) Koyama, H.; Ito, T.; Nakanishi, T.; Sekimizu, K. *Genes Cells* **2007**, *12*, 547.

(13) Brégeon, D.; Doddridge, Z. A.; You, H. J.; Weiss, B.; Doetsch, P. W. *Mol. Cell* **2003**, *12*, 959.

(14) Thomas, M. J.; Platas, A. A.; Hawley, D. K. *Cell* **1998**, *93*, 627.

(15) Jeon, C.; Agarwal, K. *Proc. Natl. Acad. Sci. U.S.A.* **1996**, *93*, 13677.

(16) Nesser, N. K.; Peterson, D. O.; Hawley, D. K. *Proc. Natl. Acad. Sci. U.S.A.* **2006**, *103*, 3268.

(17) Reines, D.; Conaway, R. C.; Conaway, J. W. *Curr. Opin. Cell Biol.* **1999**, *11*, 342.

(18) Erie, D. A.; Yager, T. D.; von Hippel, P. H. *Annu. Rev. Biophys. Biomol. Struct.* **1992**, *21*, 379.

(19) Koyama, H.; Ito, T.; Nakanishi, T.; Kawamura, N.; Sekimizu, K. *Genes Cells* **2003**, *8*, 779.

(20) Izban, M. G.; Luse, D. S. *J. Biol. Chem.* **1993**, *268*, 12864.

(21) Rudd, M. D.; Izban, M. G.; Luse, D. S. *Proc. Natl. Acad. Sci. U.S.A.* **1994**, *91*, 8057.

(22) Weilbaecher, R. G.; Awrey, D. E.; Edwards, A. M.; Kane, C. M. *J. Biol. Chem.* **2003**, *278*, 24189.

(23) Sigurdsson, S.; Dirac-Svejstrup, A. B.; Svejstrup, J. Q. *Mol. Cell* **2010**, *38*, 202.
(24) Johnson, T. L.; Chamberlin, M. J. *Cell* **1994**, *77*, 217.
(25) Awrey, D. E.; Weilbaecher, R. G.; Hemming, S. A.; Orlicky, S. M.; Kane, C. M.; Edwards, A. M. *J. Biol. Chem.* **1997**, *272*, 14747.
(26) Erie, D. A.; Hajiseyedjavadi, O.; Young, M. C.; von Hippel, P. H. *Science* **1993**, *262*, 867.
(27) von Hippel, P. H. *Science* **1998**, *281*, 660.
(28) Reines, D.; Chamberlin, M. J.; Kane, C. M. *J. Biol. Chem.* **1989**, *264*, 10799.
(29) Izban, M. G.; Luse, D. S. *J. Biol. Chem.* **1993**, *268*, 12874.
(30) Jackson, S. P.; Bartek, J. *Nature* **2009**, *461*, 1071.
(31) Tornaletti, S.; Patrick, S. M.; Turchi, J. J.; Hanawalt, P. C. *J. Biol. Chem.* **2003**, *278*, 35791.
(32) Doetsch, P. W. *Mutat. Res.* **2002**, *510*, 131.
(33) Saxowsky, T. T.; Doetsch, P. W. *Chem. Rev.* **2006**, *106*, 474.
(34) Wang, D.; Zhu, G.; Huang, X.; Lippard, S. J. *Proc. Natl. Acad. Sci. U.S.A.* **2010**, *107*, 9584.
(35) Nath, S. T.; Lee, M. S.; Romano, L. J. *Nucleic Acids Res.* **1987**, *15*, 4257.
(36) Dimitri, A.; Jia, L.; Shafirovich, V.; Geacintov, N. E.; Broyde, S.; Scicchitano, D. A. *DNA Repair (Amsterdam)* **2008**, *7*, 1276.
(37) Marietta, C.; Brooks, P. J. *EMBO Rep.* **2007**, *8*, 388.
(38) Bregeon, D.; Doetsch, P. W. *Nat. Rev. Cancer* **2011**, *11*, 218.
(39) Tornaletti, S.; Maeda, L. S.; Kolodner, R. D.; Hanawalt, P. C. *DNA Repair (Amsterdam)* **2004**, *3*, 483.
(40) Kim, T. W.; Delaney, J. C.; Essigmann, J. M.; Kool, E. T. *Proc. Natl. Acad. Sci. U.S.A.* **2005**, *102*, 15803.
(41) Kim, T. W.; Kool, E. T. *J. Org. Chem.* **2005**, *70*, 2048.
(42) Khakshoor, O.; Wheeler, S. E.; Houk, K. N.; Kool, E. T. *J. Am. Chem. Soc.* **2012**, *134*, 3154.
(43) Huang, X.; Wang, D.; Weiss, D. R.; Bushnell, D. A.; Kornberg, R. D.; Levitt, M. *Proc. Natl. Acad. Sci. U.S.A.* **2010**, *107*, 15745.
(44) Kool, E. T. *Biopolymers* **1998**, *48*, 3.
(45) Moran, S.; Ren, R. X.; Rumney, S.; Kool, E. T. *J. Am. Chem. Soc.* **1997**, *119*, 2056.
(46) Kool, E. T. *Curr. Opin. Chem. Biol.* **2000**, *4*, 602.
(47) Kim, T. W.; Brieba, L. G.; Ellenberger, T.; Kool, E. T. *J. Biol. Chem.* **2006**, *281*, 2289.
(48) Sintim, H. O.; Kool, E. T. *Angew. Chem., Int. Ed.* **2006**, *45*, 1974.
(49) Silverman, A. P.; Garforth, S. J.; Prasad, V. R.; Kool, E. T. *Biochemistry* **2008**, *47*, 4800.
(50) Wolfle, W. T.; Washington, M. T.; Kool, E. T.; Spratt, T. E.; Helquist, S. A.; Prakash, L.; Prakash, S. *Mol. Cell. Biol.* **2005**, *25*, 7137.
(51) Washington, M. T.; Helquist, S. A.; Kool, E. T.; Prakash, L.; Prakash, S. *Mol. Cell. Biol.* **2003**, *23*, 5107.
(52) Mizukami, S.; Kim, T. W.; Helquist, S. A.; Kool, E. T. *Biochemistry* **2006**, *45*, 2772.
(53) Irimia, A.; Eoff, R. L.; Pallan, P. S.; Guengerich, F. P.; Egli, M. *J. Biol. Chem.* **2007**, *282*, 36421.
(54) Doublie, S.; Tabor, S.; Long, A. M.; Richardson, C. C.; Ellenberger, T. *Nature* **1998**, *391*, 251.
(55) Spratt, T. E. *Biochemistry* **1997**, *36*, 13292.
(56) Morales, J. C.; Kool, E. T. *J. Am. Chem. Soc.* **1999**, *121*, 2323.
(57) Morales, J. C.; Kool, E. T. *Biochemistry* **2000**, *39*, 12979.
(58) Krueger, A. T.; Kool, E. T. *Curr. Opin. Chem. Biol.* **2007**, *11*, 588.
(59) Sawaya, M. R.; Prasad, R.; Wilson, S. H.; Kraut, J.; Pelletier, H. *Biochemistry* **1997**, *36*, 11205.
(60) Li, Y.; Mitaxov, V.; Waksman, G. *Proc. Natl. Acad. Sci. U.S.A.* **1999**, *96*, 9491.
(61) Huang, H.; Chopra, R.; Verdine, G. L.; Harrison, S. C. *Science* **1998**, *282*, 1669.
(62) Morales, J. C.; Kool, E. T. *Biochemistry* **2000**, *39*, 2626.
(63) Kim, T. W.; Kool, E. T. *Org. Lett.* **2004**, *6*, 3949.
(64) Khakshoor, O.; Wheeler, S. E.; Houk, K. N.; Kool, E. T. *J. Am. Chem. Soc.* **2012**, *134*, 3154.
(65) Kool, E. T. *Acc. Chem. Res.* **2002**, *35*, 936.
(66) Kireeva, M.; Nedialkov, Y. A.; Gong, X. Q.; Zhang, C.; Xiong, Y.; Moon, W.; Burton, Z. F.; Kashlev, M. *Methods* **2009**, *48*, 333.